Electronic Supplementary Information for

A UOF based on cyclotriphosphazene skeleton: fluorescent sensing of different substituted aldehyde and NACs

*Yao Xiao,[a] Zi-Xin You,[a] Qing-Lin Guan,[a] Li-Xian Sun,[b] Yong-Heng Xing,[*a] Feng-Ying Bai[*a]*

a College of Chemistry and Chemical Engineering, Liaoning Normal University, Dalian City, 116029, P.R. China.

b Guangxi Key Laboratory of Information Materials, Guilin University of Electronic Technology, Jinji Road 1#, Guilin 541004, P. R. China

Table of Contents

Materials and Methods

X-ray Crystallographic Determination

Detailed characterization

Synthesis of U-hdpcp

Coordination environment

Preparation of Fluorescent Films

Cyclic experiments

Related calculations

Figure S25 The changes of IR spectra and UV-vis spectra before and after detection of aromatic aldehydes

Figure S26 The changes of IR spectra and UV-vis spectra before and after detection of NACs
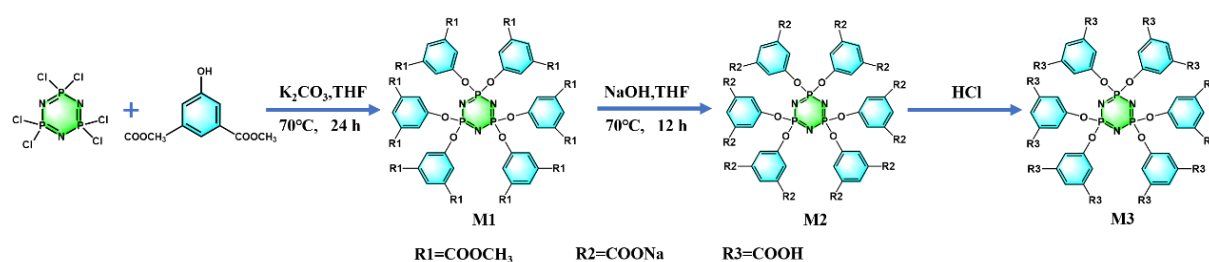
Materials and Methods: Caution! Suitable measures for precautions and protection should be taken, and all operations should follow the criteria while handling such substances although natural uranium was used in the experiment. The ligand H_{12}HDPCP was prepared by literature method and appropriately modified the methods.[1] All other original chemical reagents and solvents employed in the present work were purchased from commercial sources and used without further purification. The synthesis of H_{12}hdpcp can be mainly divided into four steps: (i) Synthesis of 5-hydroxy isophthalic acid dimethyl ester: 5.45 g of 5-hydroxyisophthalic acid was dissolved in 45 mL of methanol. After the reactant was completely dissolved, it was transferred to an ice water bath and stirred for 30 minutes. Then, 1 mL of concentrated H_2SO_4 was slowly added dropwise. Subsequently, the solution was refluxed at 72 °C for 8 hours. After the reaction is completed, it was cooled to room temperature, a saturated $NaHCO_3$ solution was added until no white precipitates. Then the white precipitate was washed and filtered to neutral. (ii) Synthesis of intermediate M1: 5-hydroxyisophthalate (3.1527 g, 15 mmol) and dry anhydrous K_2CO_3 (2.3469 g, 17 mmol) were dissolved in 40 mL of tetrahydrofuran (THF) and stirred for 15 minutes. 0.8629 g triphosphazene chloride (2.5 mmol) was dissolved in 10 mL of THF and was transferred to a constant pressure drip funnel. Then the triphosphazene chloride solution was slowly dripped into two flasks under nitrogen atmosphere. After the dripping is completed, the mixture was heated and refluxed at 70 °C for 22 hours. After stopping the reaction, THF was removed from the system by rotary evaporation, and finally obtain white intermediate M1. (iii) Synthesis of intermediate M2: The obtained intermediate M1 and 30 mL THF was added to a 100 mL two-necked flask. 2.3 g of solid sodium hydroxide (NaOH) was dissolved in 20 mL of deionized water to prepare a NaOH solution, and it was slowly added to two-necked flask. After heating and refluxing at 70 °C for 12 hours, the

reaction was stopped to obtain a layered transparent clear liquid.   The upper layer was a colorless

organic phase, and the lower layer was a light yellow aqueous phase.   The aqueous solution of M2

was obtained by rotary evaporation to remove THF.

(iv) Synthesis of H_{12}hdpcp: The M2 solution was transferred to a 500 mL beaker and concentrated hydrochloric acid was added to it, a large amount of white precipitates was precipitated.   Finally, it was washed and filtered to neutral.

| M1 | Synthesis of intermediate M2 | M2 | Hydrolysis reaction | Addition   of concentrated HCl | HDPCP |

Scheme 1 Synthesis process of ligand H_{12}hdpcp

R1=COOCH₃   R2=COONa   R3=COOH

Scheme 2 Synthetic routes of the ligand H_{12}hdpcp

X-ray Crystallographic Determination

The Bruker AXS TENSOR-27 FT-IR spectrometer was applied to record Infrared spectra in the range of 4000-400 cm^{-1}.   UV-vis absorption spectra of solid sample were received from a JASCO V-570 UV/VIS/NIR spectrophotometer with the range of 200-800 nm, and Lambda 35 spectrometer was applied to record the UV-vis absorption spectra of suspension samples in 200-800 nm. Thermogravimetric data was obtained from a PerkinElmer Diamond TG/DTA under nitrogen protection from room temperature to 1100 °C with the heating rate of 10 °C·min^{-1}.   X-ray powder diffraction (PXRD) patterns were performed on an Advance D8 equipped with Cu-Kα radiation in the range of 5° < 2θ < 60°, with a step size of 0.02° (2θ) and a count time of 2 s per step.   The HORIBA Fluoromax-4-TCSPC spectrofluorometer which is provided with Pulsed LED sources (200-1000 nm) with 3.2-inch Integrating Sphere was used to measure the fluorescence behavior of the coordination complexes at room temperature.   The size and morphology of the material surface was investigated by Scanning Electron Microscope & X-ray Analyzer (SEM, SU8010) and Atomic Force Microscope (AFM, Asylum Research Cypher ES).   The crystallographic diffraction data of U-hdpcp was measured on Bruker AXS SMART APEX II CCD diffractometer graphite monochromatized Mo Kα radiation (λ = 0.71073 Å) at 293 K and were displayed in Table S1.   The space group was determined by Olex2 platform and, all atoms were anisotropic ally refined by direct method (XL) and least-squares refinement (XS) in the final cycle.   Solvents that are crystallographically ill-defined occupied the large channels in the complexes.   The SQUEEZE

function within the PLATON 40 of programs was employed to analyze the residual electron density illustrating that there are 294 electrons in each formula unit of the U-hdpcp. This corresponds to one molecular of H_2O and seven DMF moleculars (calculated: 290 electrons). Due to the disorder of some of the atoms in the structure of U-hdpcp, we made split treatment on them, including the benzene rings and carboxyl groups of the ligand. But there are still several B level alerts in the checkCIF files. We provided reasonable explanations for these alerts. For RINTA01_ALERT_3_B and PLAT020_ALERT_3_B, it resulted from air-sensitive crystalbadly diffracting; twin; cracked after out of oil. Similar situation has also appeared in the reported literature.[2] For PLAT420_ALERT_2_B, it is because there are no reasonable acceptor atoms present in the structure that facilitate this. Similar situation was reported in the literature.[3] For PLAT910_ALERT_3_B, which is because these were lost behind the beamstop.[4] Similar situation was reported in the literature.[5]

Detailed characterization

To further characterize the structure and properties of the complex, we constructed a series of basic characterizations, including infrared spectroscopy (IR), ultraviolet visible spectroscopy (UV-vis), powder X-ray diffraction (PXRD), thermogravimetric analysis (TG) and fluorescence spectroscopy (Fig.S4-Fig.S7) The detailed crystallography data and selected bond distances and angles are listed in the Tab.S1-Tab.S2. The detailed assignments of IR and UV-vis spectroscopy were displayed in Tab.S3-Tab.S4. The PXRD pattern of as-synthesized U-hdpcp was compared with the simulation to confirm purity of the complex. To test the thermal stability of the complex, a thermogravimetric analysis was performed at a heating rate of 10 °C min^{-1} in a temperature range of 30 to 800 °C under N_2 atmosphere. The TG curve illustrated there are the three stages of weight loss. The complex remains complete until 150 °C. The first stage of weight loss from 150 °C to 300 °C corresponds to the removal of one free H_2O molecular and three free DMF molecules (theoretical value 6.91%, calculated value 7.13%). The second stage from 300 °C to 450 °C corresponds to the loss of four free DMF molecules (theoretical value 8.51%, calculated value 9.02%). The stage of collapse of framework occurred from 450 °C, which corresponded to collapse of the skeleton to remain uranium oxygen clusters and ligand fragments (about 83.85%). The solid fluorescence spectra of the ligand and complex were measured to characterize the photophysical properties of the complex (Fig.S8). The complex exhibited a strong fluorescence emission peak at 515-535 nm, which can be attributed to the combined effects of the fluorescence emission of the ligand and the electron and vibrational transfer transitions of UO_2^{2+} $S_{10}-S_{0v}$ (v= 0−4). The absence of other characteristic peaks of UO_2^{2+} may be due to the coordination environment. The photoluminescence quantum yield of U-hdpcp is 9.03%.

Synthesis of U-hdpcp: The complex U-hdpcp was prepared by solvothermal method with 0.014 g of H_{12}hdpcp (0.03 mmol) and 0.0394 g of $UO_2(NO_3)_2 \cdot 6H_2O$ (0.01 mmol) in a mixed solvent (DMF-H_2O 2:1). Next, the pH of the solution was adjusted to 3~4 with dilute HNO_3 and reacted at 160 °C for 5 days to obtain yellow crystal. The yield was 74% (based on H_{12}hdpcp). Anal. Calc. for $C_{69}H_{76}N_{10}O_{54}P_3U_6$ (%): C, 24.14; H, 2.21; N, 4.08. Found (%): C, 24.16; H, 2.20; N, 4.08. Infrared data (cm^{-1}): 3441, 3180, 1613, 1558, 1364, 1201, 1114, 1016, 898, 787.

Coordination environment: For U2, the coordination environment of it is similar to that of U4. The equatorial plane is occupied by two carboxyl oxygen atoms (O14 and O30) in the monodentate mode and three bridged oxygen atoms μ_2-O (O42) and μ_3-O (O40 and O41), and the average bond distance is 2.272(12)~2.51(3) Å. In the axial direction, U2 is bonded with O33 and O34, and the

average bond distance is 1.663(12)~1.742(15), and the bond angle of $O_t=U=O_t$ is 178.6(6)°. The coordination environment of U3 is similar to that of U1. U3 coordinates with three carboxyl oxygen atoms from the ligand (O19, O20 and O13) and two bridged oxygen atoms μ_2-O (O39) and μ_3-O (O40) to form an equatorial plane, the average bond distance is 2.238(12)~2.578(15) Å. It bonds with two oxygen atoms in the axial direction (O37 and O38) with average bond distance 1.672(12)~1.874(15) Å and the bond angle of $O_t=U=O_t$ is 176.0(5)°. The coordination environment of U5 is similar to that of U6. The equatorial plane of U5 consists of five carboxyl oxygen atoms from the ligand (O8, O11, O12, O15 and O21) with an average bond distance of 2.14(3)~2.55(2) Å (Fig. S3b). O8, O15 and O21 adopts monodentate coordination mode. O11 and O12 adopts bidentate chelated coordination mode. In the axial direction, it is occupied by O45 and O46 with an average bond distance of 1.666(14)~1.753(15) Å and the bond angle of $O_t=U=O_t$ is 176.5(6)°.

Preparation of Fluorescent Films: The method is to dissolve 1 g of polyvinyl alcohol in 150 mL of deionized water heating to 105 °C and reacting for 1.5 hours to obtain aqueous solution of polyvinyl alcohol. Next, 20 mg of U-hdpcp powder and 10 mL of PVA solution were added to a 15 mL centrifuge tube and sonicated for 1 hour to obtain a uniformly dispersed U-hdpcp@PVA suspensions (concentration: 2 mg/mL). The silicon wafers were selected as the spraying substrate and ethanol was used to ultrasonically clean for 15 min for surface cleaning. A spin coating instrument was used to spin coat U-hdpcp@PVA suspensions onto silicon wafers, with five spin coating cycles and a rotational speed of 4000 r/min. The silicon wafers were dried at 60 °C.

Cyclic experiments: To investigate the renewable ability of U-hdpcp in detecting aromatic aldehydes, we conducted cycling experiments. After each sensing experiment, we collected U-hdpcp powder after detecting aromatic aldehydes, and filtered, cleaned with ultrasound, centrifuged and dried it. Then we conducted the next fluorescence detection experiment and recorded the fluorescence intensity of U-hdpcp before and after pollutants detection. The results showed that after two circle of sensing experiments, the fluorescence intensity of U-hdpcp can recover to over 83% of its initial fluorescence intensity, which indicate that U-hdpcp can be recycled twice.

Related calculations: The quenching constants were calculated according to Stern–Volmer equation, $I_0/I-1=K_{SV}[Q]$ (where I_0 and I are the fluorescence intensity of U-hdpcp before and after dropping aldehydes, K_{SV} is the quenching constants (M^{-1}), Q is the concentration of the aldehyde solution (M)). As the concentration of aldehydes in the test solution increases, the fitting curve gradually turns to nonlinear, so we used $I_0/I=a \exp (k\,[Q])+b$ to fit the overall trend (a, k, q are constants, [Q] is the concentration of the aldehyde solution (M), I_0 and I are the fluorescence intensity of U-hdpcp before and after dropping aldehydes). The limit of detection was calculated a by LOD=$3\sigma/K_{SV}$ (where σ is relative standard deviation of eleven blank experiments).

Tab. S1 The crystallographic data of single crystal X-ray diffraction of U-hdpcp[*]

Complexes	**U-hdpcp**
Formula	$C_{69}H_{76}N_{10}O_{54}P_3U_6$
M (g mol^{-1})	3430
Crystal system	*monoclinic*
Space group	$P2_1/n$
a (Å)	21.139(3)

b (Å)	25.914(4)		
c (Å)	25.518(3)		
α (°)	90		
β (°)	109.474(4)		
γ (°)	90		
V (Å^3)	13179(3)		
Z	4		
D_{calc}	1.458		
Crystal size/mm	$0.12 \times 0.11 \times 0.1$		
$F(000)$	5168.0		
μ (Mo-Kα)/mm^{-1}	7.441		
2θ (°)	4.38~50		
Reflections collected	85596		
Independent Reflections (I >2σ(I))	23187		
Parameters	1474		
$\Delta(\rho)$ (e Å^{-3})	2.01/-2.15		
Goodness of fit	1.048		
$R_I{}^{\mathrm{a}}$, $wR_2{}^{\mathrm{b}}$ [I > 2σ(I)]	0.0780 (0.1525)$^{\mathrm{b}}$		
R_I, wR_2 (all data)	0.1634 (0.1802)$^{\mathrm{b}}$		

*$^{\mathrm{a}}$R$_1$=Σ||Fo|−|Fc||/Σ|Fo|, wR$_2$=[Σw(Fo^2–Fc^2)^2/Σw(Fo^2)^2]$^{1/2}$; [Fo>4σ(Fo)]$^{\mathrm{b}}$, where w = 1/σ^2(F$_o{}^2$), based on all data

Tab. S2 Selected bond distances (Å) and bond angle (°) for **U-hdpcp***

U(1)$^{\#1}$-O(17)	2.56(2)	U(1)$^{\#1}$-O(18)	2.50(3)
U(1)$^{\#3}$-O(24)	2.36(2)	U(1)-O(31)	1.629(16)
U(1)-O(32)	1.744(13)	U(1)-O(41)	2.203(11)
U(1)-O(42)	2.330(14)	U(2)$^{\#2}$-O(14)	2.48(3)
U(2)$^{\#2}$-O(30)	2.30(4)	U(2)-O(33)	1.742(15)
U(2)-O(34)	1.663(12)	U(2)-O(40)	2.272(12)
U(2)-O(41)	2.313(11)	U(2)-O(42)	2.443(11)
U(3)$^{\#2}$-O(13)	2.54(3)	U(3)-O(19)	2.559(15)
U(3)-O(20)	2.549(14)	U(3)-O(37)	1.874(15)
U(3)-O(38)	1.672(12)	U(3)-O(39)	2.308(12)
U(3)-O(40)	2.238(12)	U(4)-O(10)$^{\#2}$	2.342(16)
U(4)$^{\#3}$-O(23)	2.453(18)	U(4)-O(35)	1.820(14)

U(4)-O(36)	1.596(13)	U(4)-O(39)	2.405(11)
U(4)-O(40)	2.285(12)	U(4)-O(41)	2.275(11)
U(5)-O(8)	2.259(15)	U(5)-O(11)	2.41(3)
U(5)-O(12)	2.55(2)	U(5)$^{\#3}$-O(15)	2.34(2)
U(5)-O(21)$^{\#2}$	2.14(3)	U(5)-O(45)	1.666(14)
U(5)-O(46)	1.753(15)	U(6)$^{\#8}$-O(16)	2.16(3)
U(6)-O(22)$^{\#6}$	2.42(2)	U(6)-O(25)	2.487(13)
U(6)-O(26)	2.433(13)	U(6)$^{\#6}$-O(28)	2.34(4)
U(6)-O(43)	1.586(15)	U(6)-O(44)	1.781(13)
O24$^{\#3}$-U1-O18$^{\#7}$	128.1(8)	O31-U1-O32	176.8(5)
O17$^{\#7}$-U1-O41	153.0(7)	O18$^{\#7}$-U1-O41	146.6(7)
O24$^{\#3}$-U1-O42	156.4(6)	O17$^{\#7}$-U1-O42	128.5(7)
O14$^{\#5}$-U2-O42	136.1(7)	O33-U2-O34	178.6(6)
O40-U2-O30$^{\#5}$	147.6(10)	O40-U2-O42	139.0(4)
O41-U2-O14$^{\#5}$	152.6(7)	O41-U2-O30$^{\#5}$	141.6(10)
O13$^{\#5}$-U3-O19	129.5(9)	O13$^{\#5}$-U3-O39	152.8(7)
O37-U3-O38	176.0(5)	O39-U3-O20	129.0(7)
O40-U3-O19	149.2(6)	O40-U3-O20	157.9(7)
O35-U4-O36	174.0(6)	O39-U4-O23$^{\#2}$	138.2(5)
O40-U4-O10$^{\#2}$	141.2(5)	O40-U4-O23$^{\#2}$	151.7(6)
O41-U4-O10$^{\#2}$	149.0(5)	O41-U4-O39	138.9(4)
O8$^{\#2}$-U5-O12	124.3(5)	O8$^{\#2}$-U5-O21$^{\#3}$	161.0(7)
O15$^{\#2}$-U5-O11	147.5(9)	O15$^{\#2}$-U5-O12	157.4(9)
O21$^{\#3}$-U5-O11	128.1(9)	O45-U5-O46	176.5(6)
O16$^{\#8}$-U6-O26	127.5(8)	O16$^{\#8}$-U6-O28$^{\#6}$	154.5(12)
O22$^{\#6}$-U6-O25	153.9(8)	O22$^{\#6}$-U6-O26	147.5(8)
O28$^{\#6}$-U6-O25	126.5(11)	O43-U6-O44	174.7(6)

#1:1/2+X,3/2-Y,-1/2+Z; #2:1/2-X,-1/2+Y,3/2-Z; #3:1-X,1-Y,2-Z; #4:3/2-X,1/2+Y,3/2-Z; #5:1/2-X,1/2+Y,3/2-Z; #6:1-X,1-Y,1-Z; #7:-1/2+X,3/2-Y,1/2+Z; #8: 3/2-X,-1/2+Y,3/2-Z

Tab.S3 The U-O bond distances of UOFs reported in some literatures (Å)

$U=O_t$	U-O ($\mu2$)	U-O ($\mu3$)	References
1.692~1.713			7
1.733~1.817	2.451~2.627	2.221~2.295	8
1.754~1.776			9
1.68~1.78			10
1.736~1.753			11
1.586~1.874	2.308~2.443	2.203~2.313	**This work**

Tab.S4 The detailed IR assignments of ligand H_{12}hdpcp and U-hdpcp (cm^{-1})

samples	ν_{O-H}	ν_{asCOO^-}	$\nu_{C=C}$	ν_{sCOO^-}	$\nu_{P=N}$	ν_{Ar-O-P}	ν_{P-N}	δ_{C-H}
H_{12}hdpcp	2747-3690	1693	1596	1415	1061-1352	999	808	781
U-hdpcp	2739-3659	1613	1558	1364	1069-1294	995	797	766

Tab. S5 The UV-vis spectra identification of ligand H12hdpcp and compound

samples	λ/nm	λ/nm	λ/nm
H_{12}hdpcp	253($\pi\rightarrow\pi^*$, H_{12}hdpcp)	301($n\rightarrow\pi^*$, H_{12}hdpcp)	—
U-hdpcp	212~545($\pi\rightarrow\pi^*$,H_{12}hdpcp)		—
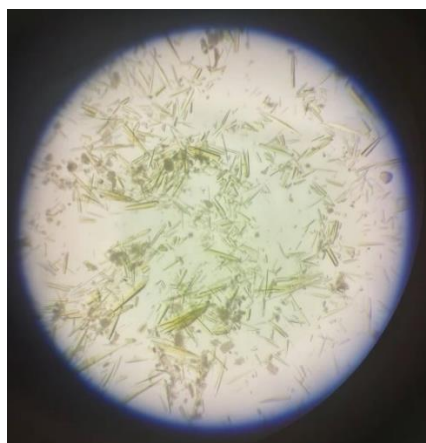
Fig. S1 Crystal shape of U-hdpcp
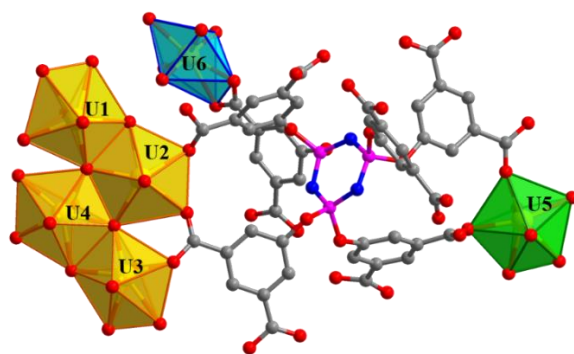
Fig. S2 The asymmetric unit of U-hdpcp
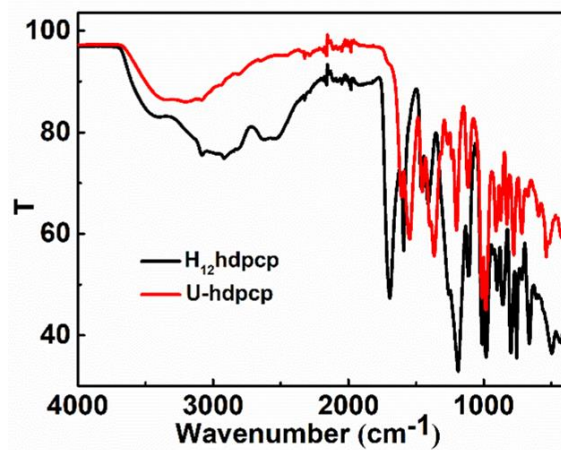
Fig. S3 Infrared spectra of H_{12}hdpcp and U-hdpcp
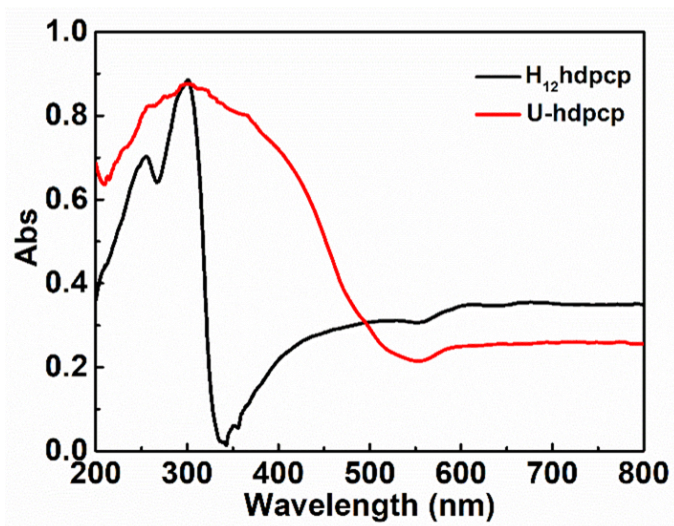
Fig. S4 The UV-vis spectra of H_{12}hdpcp and U-hdpcp
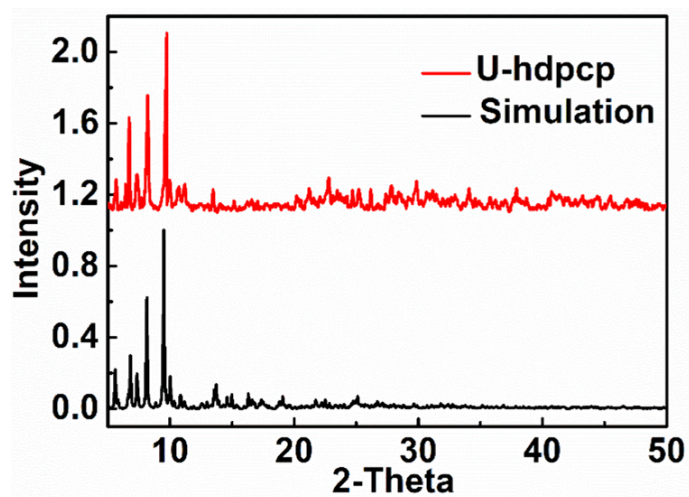
Fig. S5 PXRD patterns of H$_{12}$hdpcp and U-hdpcp
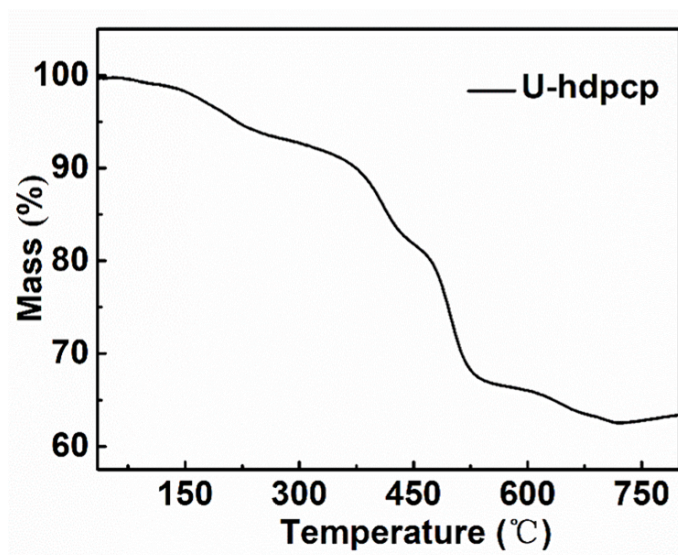
Fig. S6 TG curve of U-hdpcp
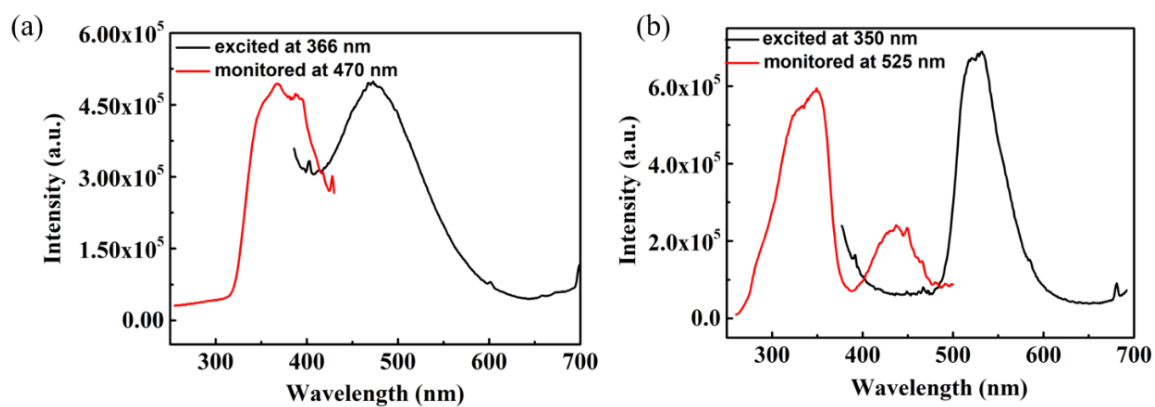
Fig. S7 The excitation and emission spectra: (a) H$_{12}$hdpcp; (b) U-hdpcp

Excitation / Scatter — **Emission / Fluorescence**

Enter Start and End Wavelengths — Enter Start and End Wavelengths

Start Wavelength	353.020	Area Balance Factor	Start Wavelength	378.060
End Wavelength	363.050	100	End Wavelength	695.960

Area	Err		Area	Err
La 1.15E+06	1074.48095		Ea 4.31E+07	65.67657
Lc 4.33E+06	2080.63753		Ec 1.45E+07	38.03463

Sample Source: DfltEm5G
Blank Source: DfltEm2G

Quantum Yield	9.03
Abs Error?	0.007
Relative Err ?	7.3765E-4

HORIBA

Fig. S8 The fitting curve of photoluminescence quantum yield of U-hdpcp
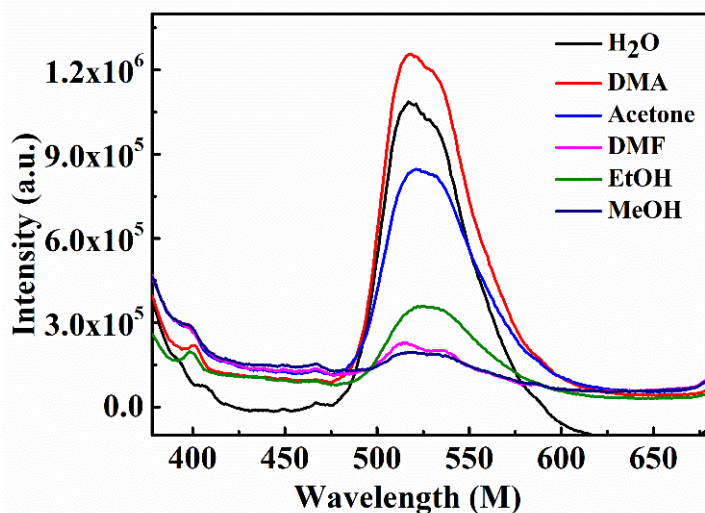
Fig. S9 Fluorescence spectra of U-hdpcp in different solvents
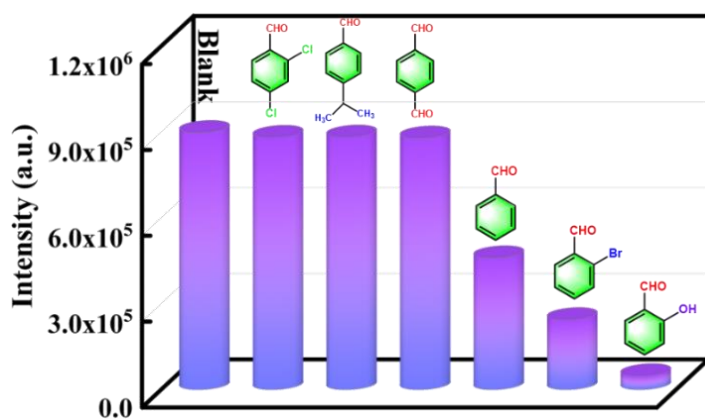
Fig. S10 The effect of different aromatic aldehydes on the fluorescence intensity of U-hdpcp
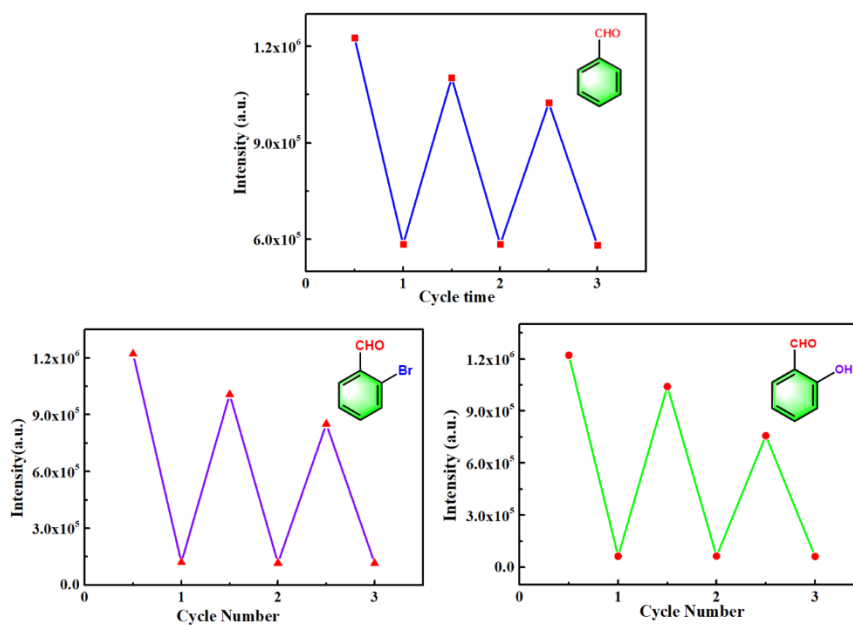
Fig. S11 Recyclability test of U-hdpcp detecting of aromatic aldehyde
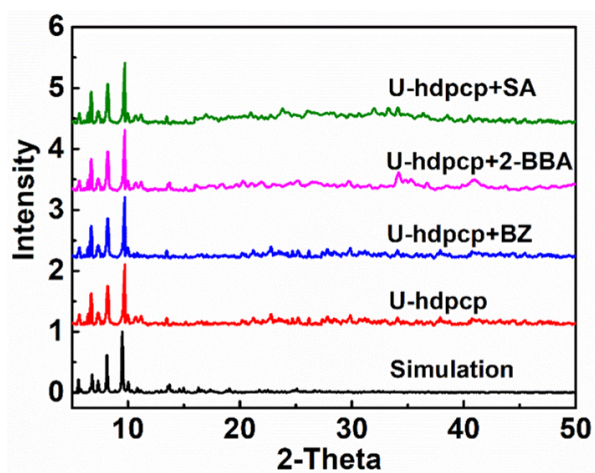
Fig. S12 The PXRD patterns of U-hdpcp after detection of aromatic aldehyde solutions
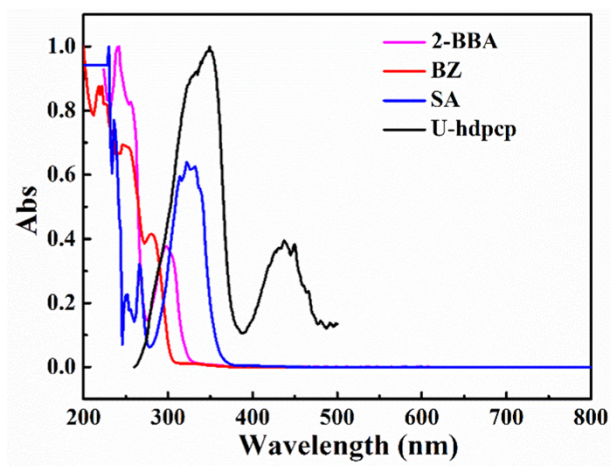
Fig. S13 Excitation spectra of U-hdpcp and UV absorption spectra of aromatic aldehydes
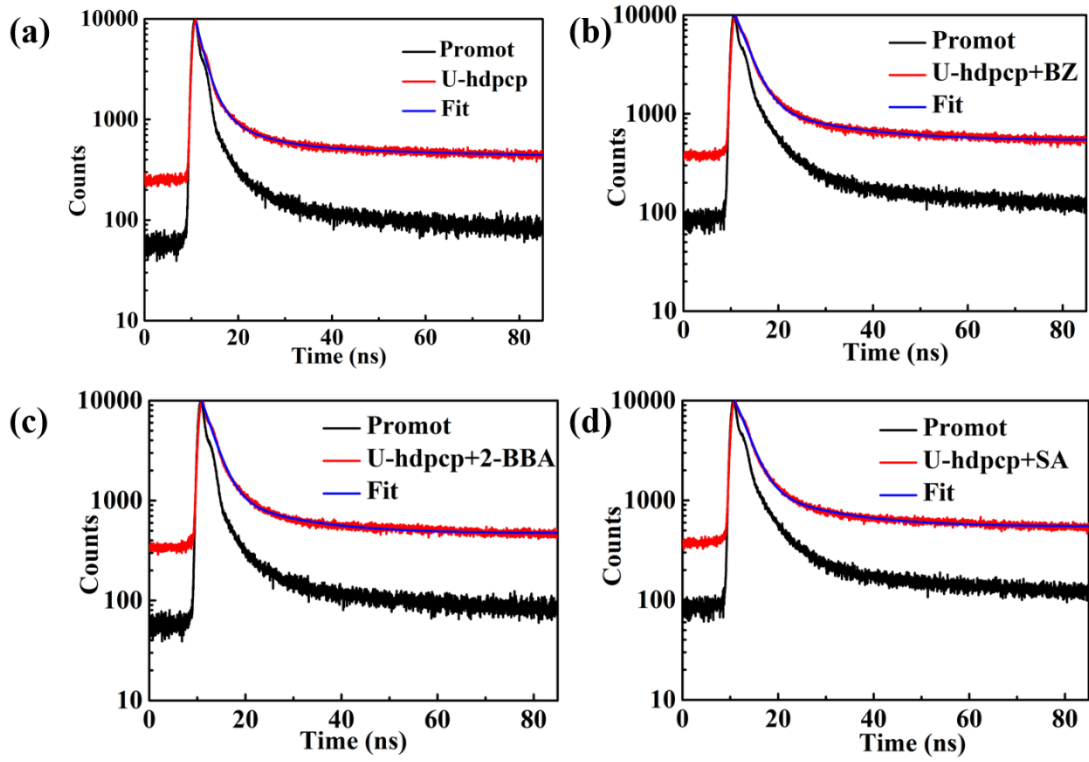
Fig. S14 The fluorescence lifetime curve of U-hdpcp before and after detecting aldehydes
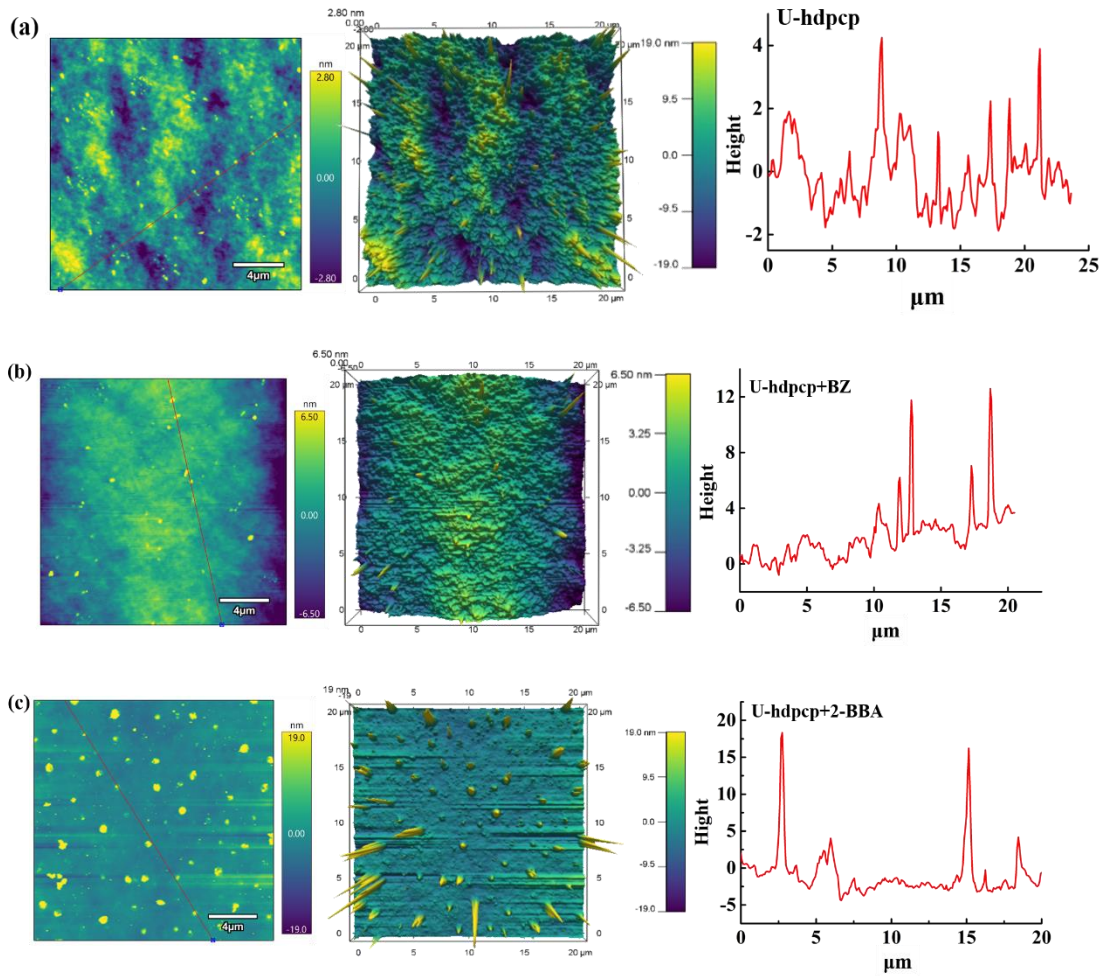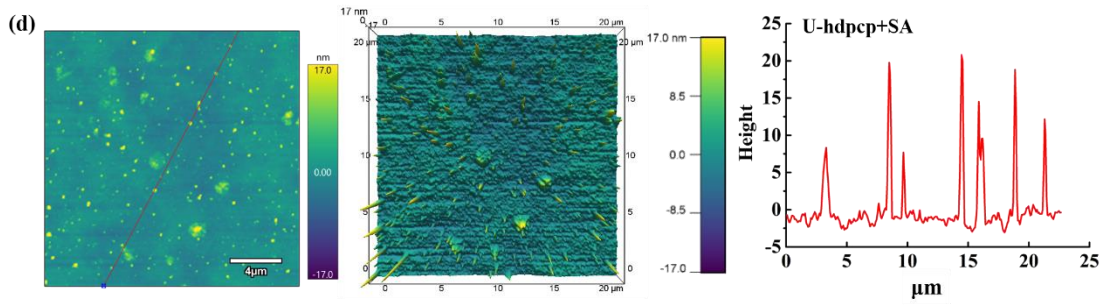
Fig. S15 AFM images of U-hdpcp before and after detection of aromatic aldehyde solutions
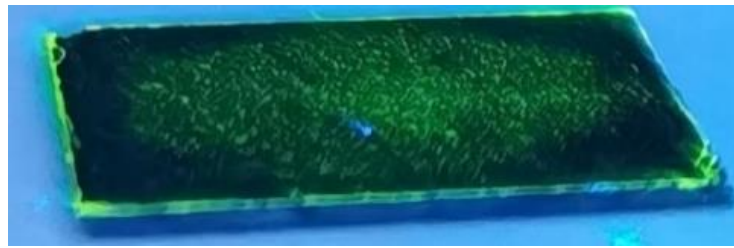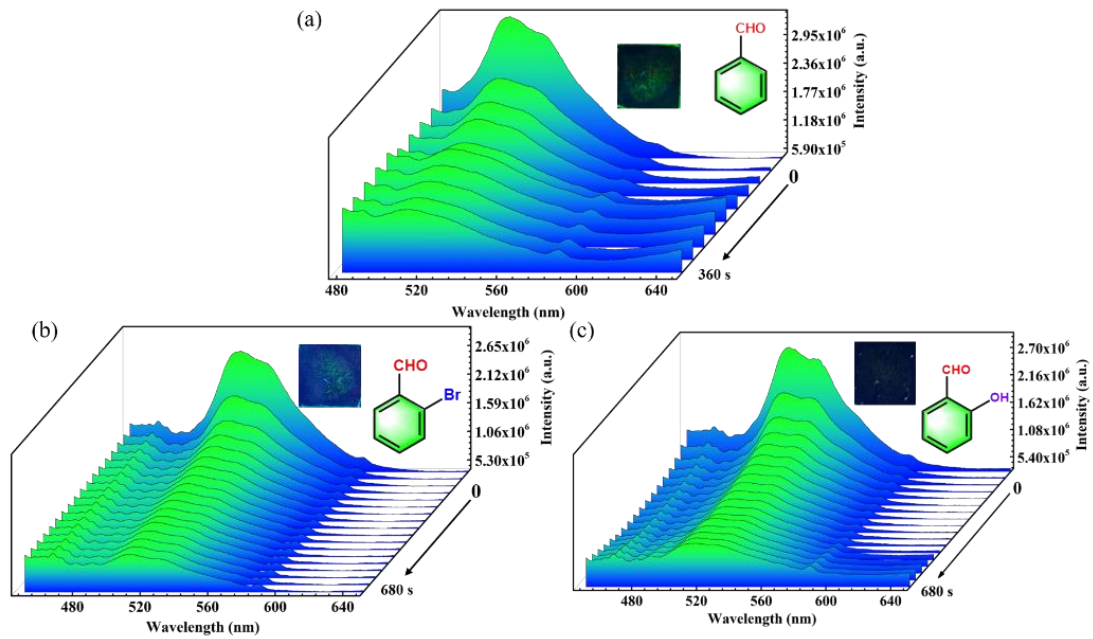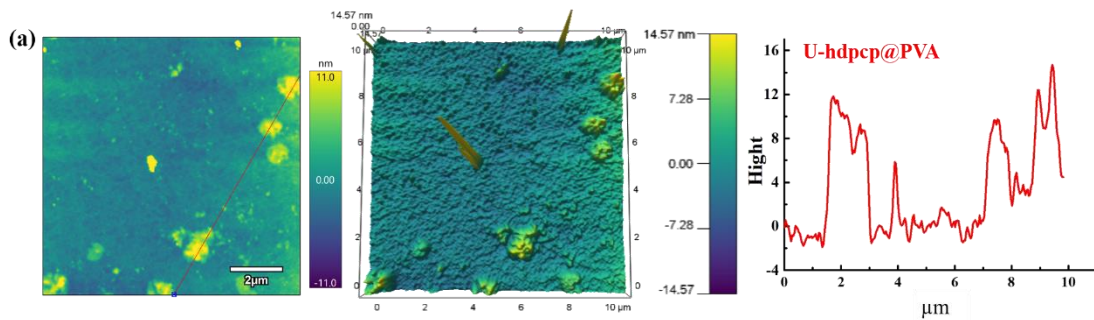

Fig. S16 Fluorescent film based on U-hdpcp@PVA

Fig. S17 Fluorescence emission spectrogram of U-hdpcp@PVA fluorescent film for detection of aromatic aldehyde vapors
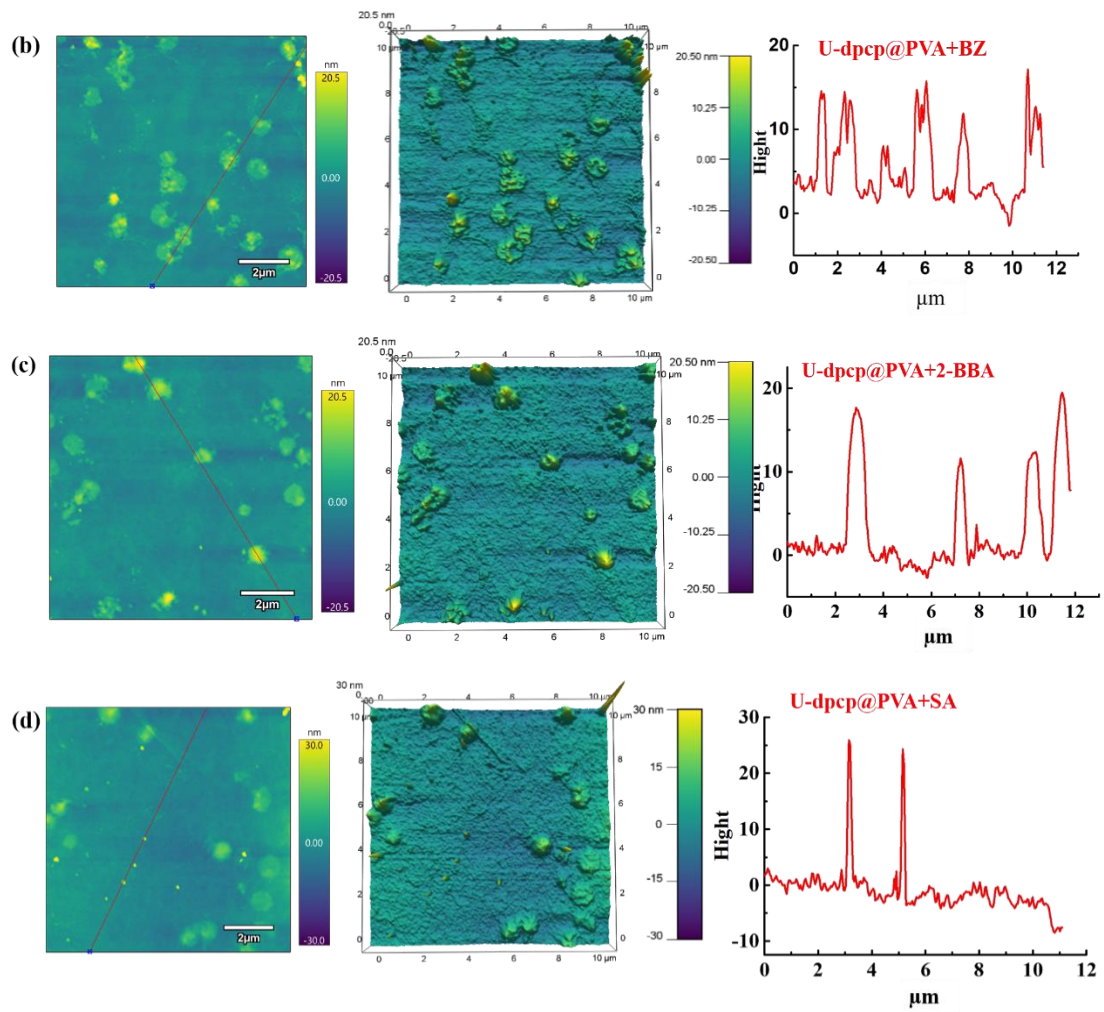
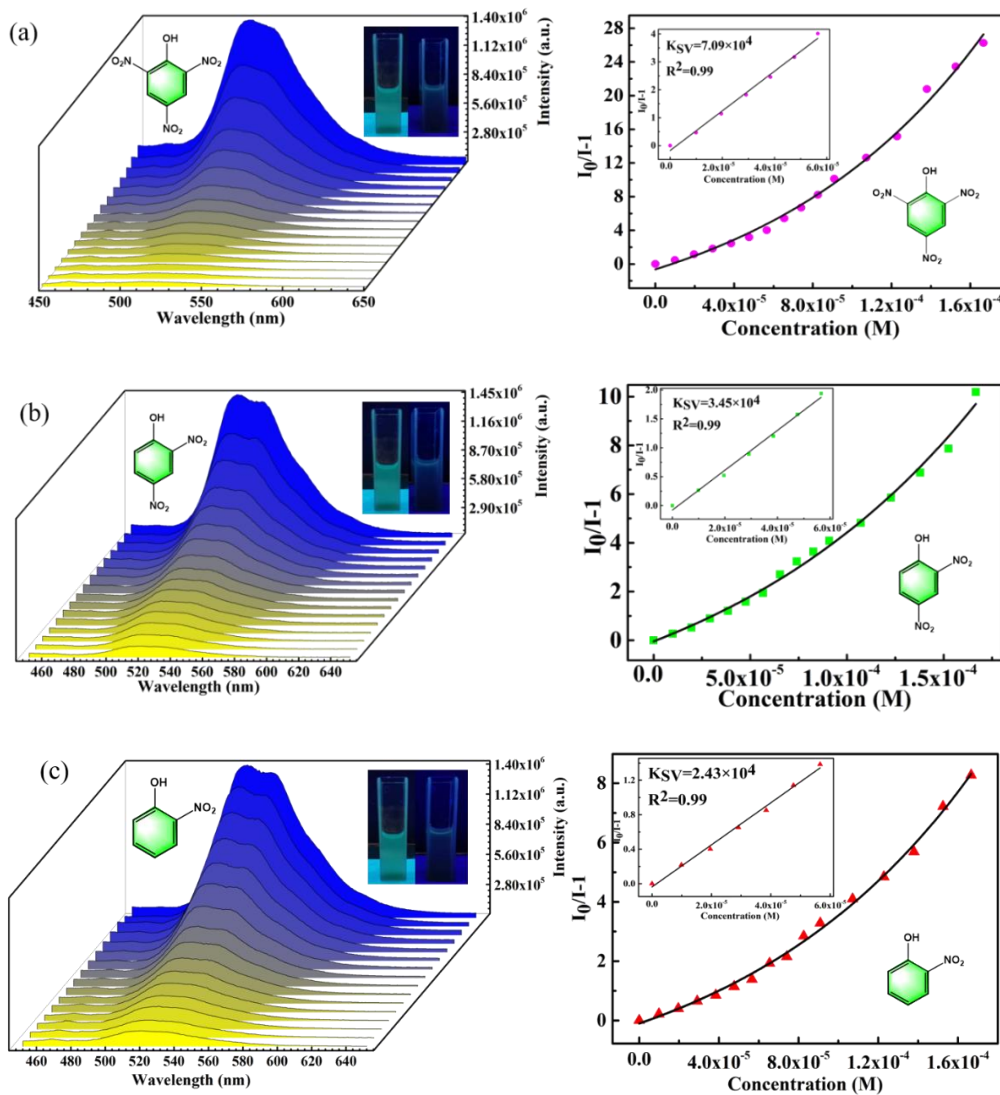Fig. S18 AFM images of U-hdpcp@PVA fluorescent film before and after detection of aromatic aldehyde vapors
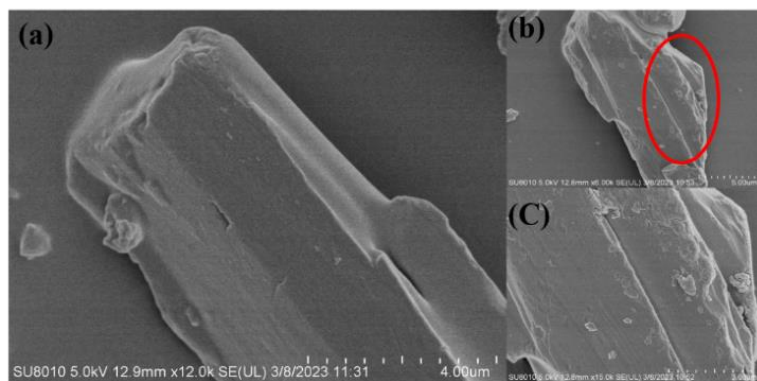
Fig. S19 SEM images of U-hdpcp @PVA fluorescent film before (a) and after detection of SA vapor (b), (c)

Fig. S20 Fluorescence emission spectra of U-hdpcp in 10^{-3} M aromatic aldehydes of titration experiment: (a) TNP; (c) DNP; (e) ONP; S-V linear diagram: (b) TNP; (d) DNP; (f) ONP.
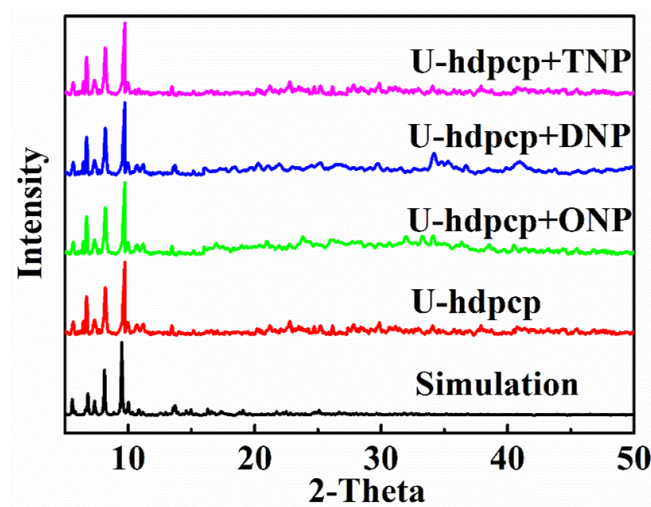

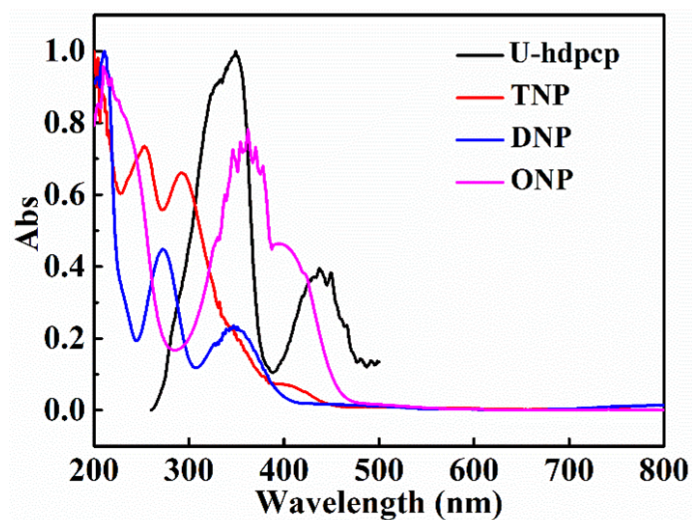Fig. S21 The PXRD patterns of U-hdpcp after detection of NACs

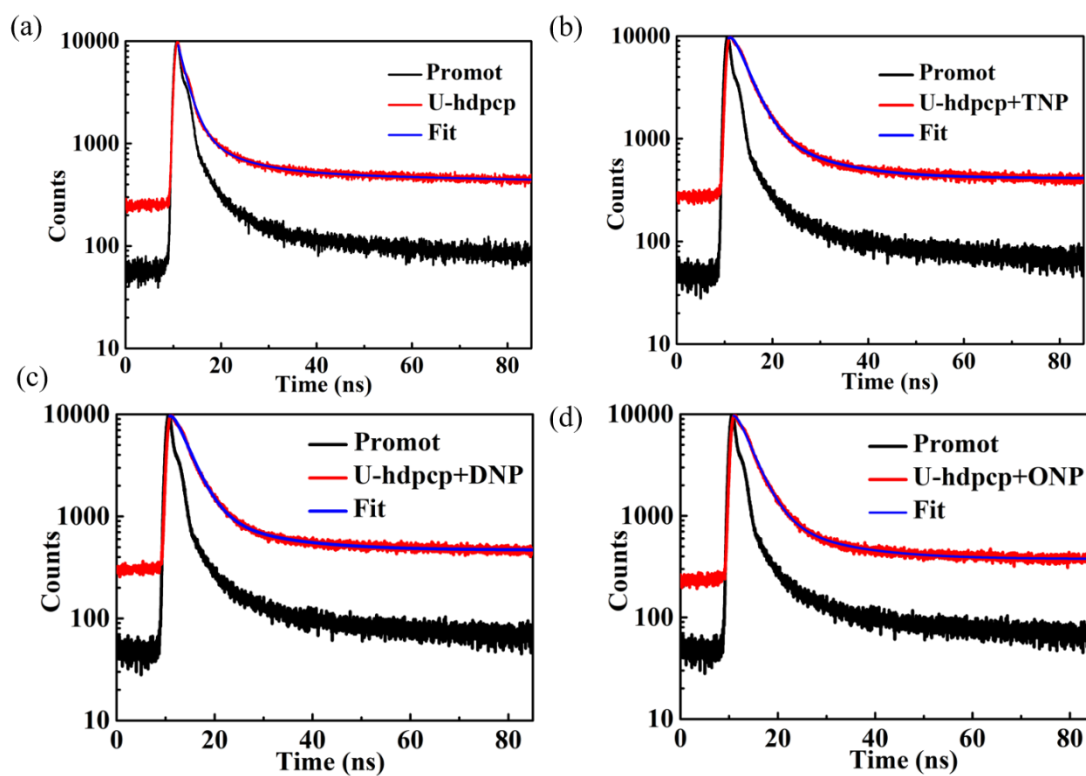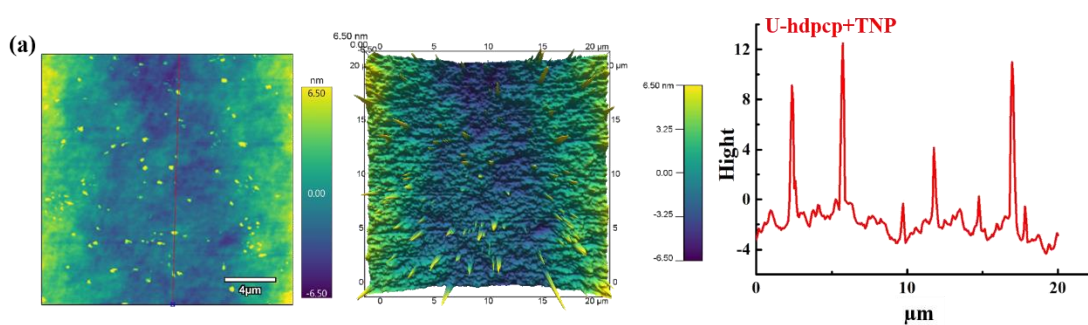Fig. S22 Excitation spectra of U-hdpcp and UV absorption spectra of aromatic aldehydes

Fig. S23 The fluorescence lifetime curve of U-hdpcp before and after detecting NACs
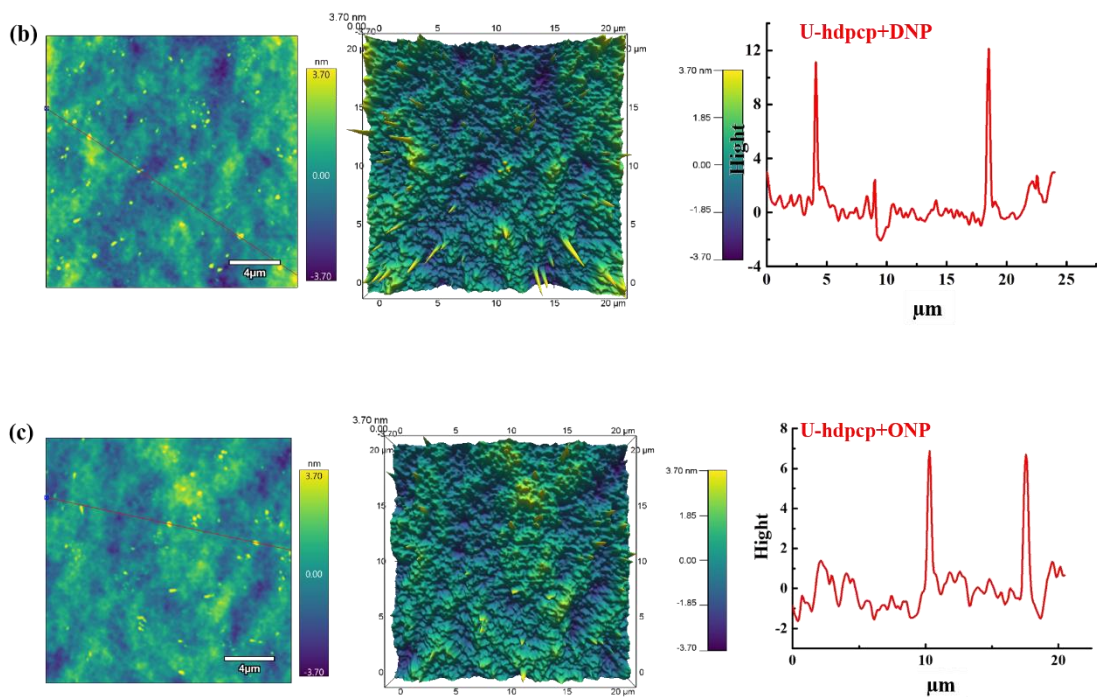
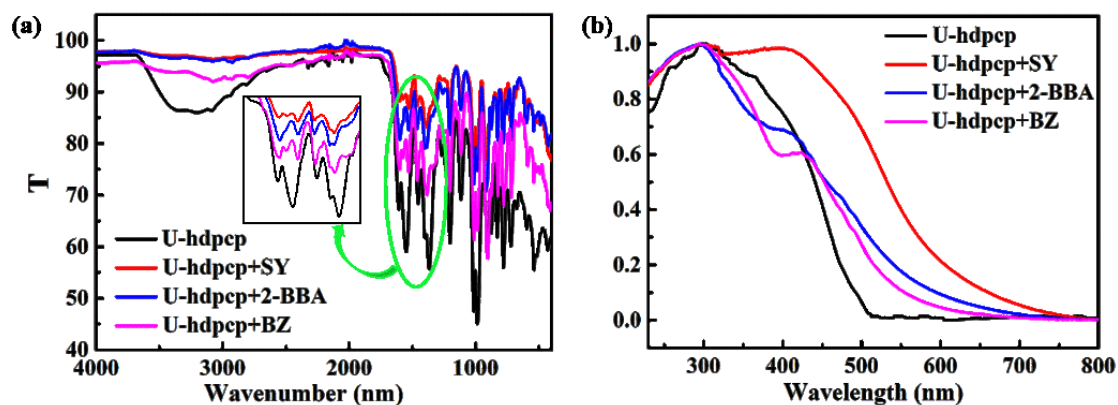Fig. S24 AFM images of U-hdpcp before and after detection of NACs

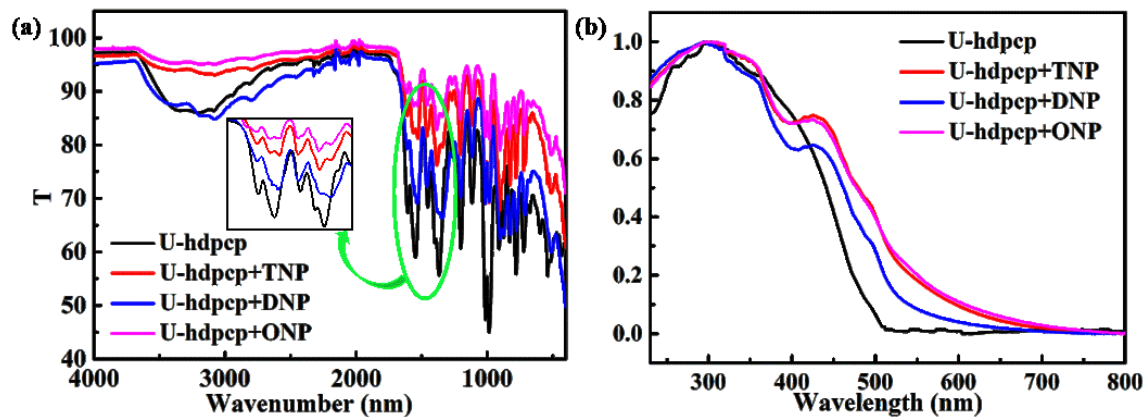Fig. S25 The changes of IR spectra (a) and UV-vis spectra (b) before and after detection of aromatic aldehydes

Fig. S26 The changes of IR spectra (a) and UV-vis spectra (b) before and after detection of NACs

References

1 Y. Ling, H. Liu, J. Jiao, Y. Feng and Y. He, ChemPlusChem, 2016, 81, 786-791.

2 J. Weihermüller, S. Schlamp, W. Milius, F. Puchtler, J. Breu, P. Ramming, S. Hüttner, S. Agarwal, C. Göbel, M. Hund, G. Papastavrou and B. Weber, J Mater Chem C, 2019, 7, 1151-1163.

3 M. J. Cliffe, E. N. Keyzer, A. D. Bond, M. A. Astle and C. P. Grey, Chem Sci, 2020, 11, 4430-4438.

4 P. J. Fischer, S. Senthil, J. T. Stephan, M. L. Swift, M. D. Storlie, E. T. Chan, M. V. Vollmer and V. G. Young, Dalton Trans, 2018, 47, 6166-6176.

5 P. J. Fischer, S. Senthil, J. T. Stephan, M. L. Swift, M. D. Storlie, E. T. Chan, M. V. Vollmer and V. G. Young, Dalton Trans, 2018, 47, 6166-6176.

6 K. Q. Hu, X. Jiang, C. Z. Wang, L. Mei, Z. N. Xie, W. Q. Tao, X. L. Zhang, Z. F. Chai and W. Q. Shi, Chemistry, 2017, **23**, 529-532.

7 S.-w. An, L. Mei, K.-q. Hu, C.-q. Xia, Z.-f. Chai and W.-q. Shi, Chem Commun, 2016, **52**, 1641-1644.

8 Y. Wang, Z. Liu, Y. Li, Z. Bai, W. Liu, Y. Wang, X. Xu, C. Xiao, D. Sheng, J. Diwu, J. Su, Z. Chai, T. E. Albrecht-Schmitt and S. Wang, J. Am. Chem. Soc., 2015, **137**, 6144-6147.

9 G. Che, D. Gu, W. Yang, M. Li and Q. Pan, *Crystal Growth & Design*, 2022, **22**, 1984-1990.

10 C. Liu, F.-Y. Chen, H.-R. Tian, J. Ai, W. Yang, Q.-J. Pan and Z.-M. Sun, Inorg. Chem., 2017, **56**, 14147-14156.